American Journal of Materials Science and Engineering, 2013, Vol. 1, No. 2, 24-28
Available online at http://pubs.sciepub.com/ajmse1/2/2

DOI:10.12691/ajmse-1-2-2

Superconductivity in Amorphous and Fully Crystallized Ni-Fe-Zr Metallic Glasses

F. Hamed*

Department of physics, Faculty of Science, United Arab Emirates University, Al-Ain, UAE
*Corresponding author: FHamed@uaeu.ac.ae

Received December 28, 2012; Revised May 03, 2013; Accepted May 05, 2013

Abstract Nano crystallization of $Ni_{0.5}Fe_{0.5}Zr_3$ metallic glasses was achieved by isothermal annealing over the temperature range 673-1173K. The crystallization precedes with the formation of metastable fcc ($FeZr_2$+$NiZr_2$) + stable bct ($FeZr_2$+$NiZr_2$) to stable bct ($FeZr_2$+$NiZr_2$). The resistivity (ρ) of the amorphous and fully crystallized states of $Ni_{0.5}Fe_{0.5}Zr_3$ metallic glasses was investigated over the temperature range 2-300k. The temperature dependence of the resistivity (ρ(T)) for the amorphous state is well described by the Mizutani's equation as group 4 metallic glasses with the Fermi level in the d band; while ρ(T) for the fully crystallized states show a negative deviation from linearity. The amorphous and crystalline states have displayed superconductive transitions at low temperatures. Enhancement in the superconducting transition temperature (T_c) in comparison to the amorphous state was observed in the fully crystallized states.

Keywords: *metallic glasses, crystallization, nano crystallization, electrical transport*

1. Introduction

The properties of Zr-based metallic glasses vary from superconducting to ferromagnetic [1,2]. Mizutani has classified metallic glasses into five groups based on their electronic properties [3]. Non-magnetic metallic glasses were classified as groups 4 and 5. Group 4 metallic glasses are defined as those for which the Fermi level is in the d band, while the Fermi level for group 5 is in the sp band. The temperature dependence of the resistivity ($\rho(T)$) of group 5 metallic glasses over the temperature range 30-300K can be understood within the framework of the generalized Faber-Ziman theory [3,4]. While for group 4 metallic glasses over the range 30-300K, Mizutani proposed the following empirical equation $\rho(T)/\rho(300K) = A + Bexp(-T/\Delta)$, where A, B and Δ are fitting parameters [4]. At temperatures below 30K, superconductivity and quantum interference effects arise [5,6,7,8]. Sabouri-Ghomi *et al* have found that the thermal annealing of Fe_xZr_{100-x} (x =20-24) metallic glasses at temperatures below the crystallization temperature (T_x) resulted in 10% enhancement in the superconducting transition temperature (T_c) [9]. While Fe_xZr_{100-x} metallic glasses are still in the amorphous state but thermally relaxed, they attributed the enhancement in T_c to the decrease of the spin fluctuation mass enhancement factor (λ_{sf}) in the modified McMillan equation [10]. Kokanović *et al* have found similar enhancement in T_c in thermally relaxed $Co_{0.2}Zr_{0.8}$ metallic glass [11]. However; he has also found that T_c decreased upon thermal annealing of $Ni_{0.24}Zr_{0.76}$ in contrast to Fe_xZr_{100-x} and $Co_{0.2}Zr_{0.8}$ metallic glasses [12]. In the above mentioned studies [9,11,12], the thermal relaxation was achieved by different heating rates up to temperatures close to T_x which resulted in partially crystallized states in a matrix of thermally relaxed amorphous state. In these studies, the enhancement in T_c was attributed to the thermally relaxed amorphous states of Fe_xZr_{100-x} and $Co_{0.2}Zr_{0.8}$ while the decrease in T_c of the thermally annealed $Ni_{0.24}Zr_{0.76}$ metallic glass was attributed to the crystallites within the matrix of the thermally relaxed amorphous state. In the present study, we will show that the isothermal annealing of $Ni_{0.5}Fe_{0.5}Zr_3$ metallic glasses for a period of two hours at temperatures beyond T_x has resulted in fully crystallized metallic states without the presence of any amorphous state. At first, the fully crystallized states have shown an enhancement in T_c compared to the amorphous state then followed by a decrease in T_c. A fully crystallized Ni-Fe-Zr metallic glass is expected to form crystallites with different sizes and phases. These phases are expected to be made up of combinations of Ni, Fe and Zr. Elemental Fe and Ni do not superconduct, while elemental Zr has a T_c of 0.6K [13]. The intermetallic crystalline C16 compounds bct Zr_2Ni and Zr_2Fe display superconductivity at 1.58K and 0.17K respectively [14,15,16]. The observed enhancement in T_c for the fully crystallized states is higher than the above values. We will argue that the observed enhancement in T_c is due to the presence of meta stable phases of fcc Zr-Ni-Fe phases. Moreover; the temperature dependence of the resistivity of the fully crystallized states where enhancement in T_c was observed show a negative deviation from linearity that resembles the behavior of the A15 compounds [17].

2. Materials and Methods

The Zr-Ni-Fe alloy ingots were prepared by arc-melting appropriate amounts of high purity (99.99%) constituent elements (75% Zr, 12.5% Ni, and 12.5% Fe) in a water-

cooled copper hearth with Zirconium getter under Argon atmosphere. The resultant ingots (1.5 grams) were melt-spun under 40Kpa Argon atmosphere on the surface of a solid 4-inch copper wheel rotating with tangential speed of 35m/s. The resultant ribbons were typically 1m long, 1mm wide and 20μm thick. The amorphous nature of the obtained ribbons was studied by Cu Kα X-ray diffraction. The ribbons were deemed to be amorphous based on the absence of diffraction peaks. A Jeol JSM-5600 scanning electron microscope equipped with Oxford EDX was used to determine the morphology, elemental composition and homogeneity of the samples. The composition of the produced metallic glass was found to be 75% Zr, 12.5% Ni, and 12.5% Fe. Differential scanning calorimetry (DSC) analyses were carried out in Perkin-Elmer DSC7 under Helium atmosphere at a heating rate of 20K/min. 5 to 7cm long ribbons of the $Ni_{0.5}Fe_{0.5}Zr_3$ metallic glass were sealed in evacuated quartz ampoules. The sealed ampoules were annealed inside a Thermolyne 1300 furnace at different temperatures for two hours. X-ray diffraction analyses were performed on the annealed samples to determine the nature of their crystalline state. Four-point resistivity measurements were performed over the temperature range 2-300K in Quantum Design PPMS model 6000.

3. Results

Figure 1 is a DSC trace of the $Ni_{0.5}Fe_{0.5}Zr_3$ metallic glass performed at a heating rate of 20K/min. The trace clearly shows one sharp exothermal peak at 660K which is taken as the crystallization temperature (T_x); annealing above T_x starts the crystallization process of the metallic glass. In this study, the $Ni_{0.5}Fe_{0.5}Zr_3$ metallic glasses were annealed for two hours at a constant temperatures (673K, 1073K and 1173K) above T_x. At such annealing temperatures, the metallic glass is expected to be fully crystallized. Figure 2 shows X-ray diffraction profiles for the amorphous and crystallized states of the metallic glasses. The X-ray diffraction profile for the amorphous state shows the usual hump seen for metallic glasses and no diffraction peaks, while the X-ray diffraction profiles for the crystallized states show strong diffraction peaks. This is a clear sign that the annealed metallic glasses are fully crystallized. The diffraction peaks can be identified with different crystalline phases. The broadening of the diffraction peaks is an indication of small grain sizes. In accordance with the Scherrer formula, the grain sizes would vary anywhere between 30 and 70nm. This suggests that the fully crystallized metallic glasses are composed entirely of large number of nano-crystallites of different phases.

Figure 3a and 3b is a plot of the normalized resistivity (ρ (T) /ρ (300K)) versus temperature for the amorphous and crystallized states of the $Ni_{0.5}Fe_{0.5}Zr_3$ metallic glass. The amorphous state has small negative temperature coefficient of resistivity; α ($\alpha = (1/\rho)\partial\rho/\partial T$). The temperature dependence of the resistivity for the amorphous state can be fitted to the following empirical equation proposed by Mizutani [4]: $\rho(T)/\rho(300K) = A + B\ exp(-T/\Delta)$, where ρ (300K) is the resistivity at 300K and A, B and Δ are fitting parameters. This equation is considered for metallic glasses which contain d electrons at the Fermi energy level, E_F. For the data fitted over the temperature range 30-300K, A is approximately unity, B ~ 0.036, and Δ = 232K. Mizutani had correlated Δ to the Debye temperature (θ_D) [5]; our fitted value for Δ compares quite well with values for Ni-Zr and Fe-Zr metallic glasses [18]. The room temperature resistivity in the amorphous state was measured to be 165μΩcm, while it dropped drastically to about 60μΩcm for the fully crystallized states. In contrast to the amorphous state, ρ (T) for the fully crystallized state decreases with temperature. ρ (T) for the 673K and 1073K annealed samples behave almost the same and show negative deviation from linearity above 45K. This behavior resembles the saturation phenomenon observed in Chevrel phases and A15 compounds [17]. The fully crystallized state is composed of a large number of nano-crystallites of different sizes and different phases and mostly likely each type of nano-crystallite may have a different $\rho(T)$. The observed ρ (T) is the combined ρ (T)'s of all the nano-crystallites where some may display saturation phenomenon behavior like. To investigate if the deviation from linearity is arising from tunneling effects at the boundaries between the nano-crystallites, we carried out Current-Voltage (I-V) measurements at different temperatures. The resulting I-V curves displayed ohmic behavior. This made us convinced that the observed behavior of ρ (T) is characteristic of the nano-crystallites in the fully crystallized state. Below 45K ρ (T) plateaus down to the residual resistivity at 4K before the superconductive transition takes place. The Figure 3b clearly shows the superconductive transitions for the amorphous and crystallized states. T_c was determined as the midway point on the resistive transitions and it was found to be 2.77K for the amorphous state and 3.29, 2.97 and 2.23K for the 673, 1073 and 1173K annealed samples respectively. A clear enhancement in T_c for the 673 and 1073K annealed samples in comparison to the amorphous state. The superconductive transition for the amorphous state is quite sharp in comparison to the amorphous state to the annealed samples. The superconductive transition for the fully crystallized state is wider with transition width of about 120mK. The onset resistive transition to the superconducting state is rather round which may indicate fluctuations in the superconducting order parameter. These fluctuations may have resulted from variations in the different nano-crystallites. These nano-crystallites may have different sizes, different phases and possibly slightly different T_c's. The existence of any amorphous phases is ruled out since the initial $Ni_{0.5}Fe_{0.5}Zr_3$ metallic glasses were annealed at temperatures above T_x for a sufficient period of time to crystallize the whole amorphous state.

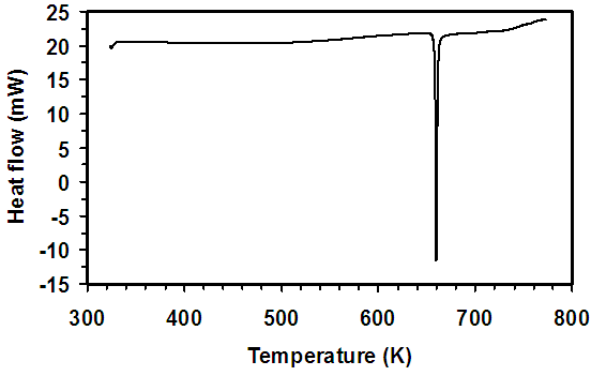

Figure 1. DSC trace of the $Ni_{0.5}Fe_{0.5}Zr_3$ metallic glass performed at a heating rate of 20K/min

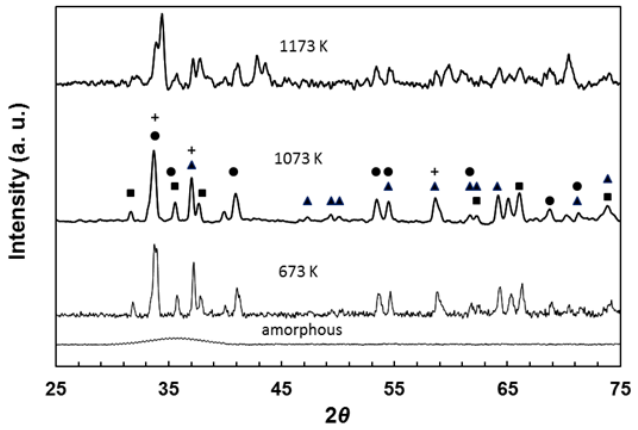

Figure 2. X-ray diffraction (XRD) profiles for different samples of Ni0.5Fe0.5Zr3 metallic glass annealed over the temperature range 763 to 1173K for a period of two hours. (▲) fcc FeZr2 and NiZr2, (■) bct FeZr2, (●) bct NiZr2, (+) Zr

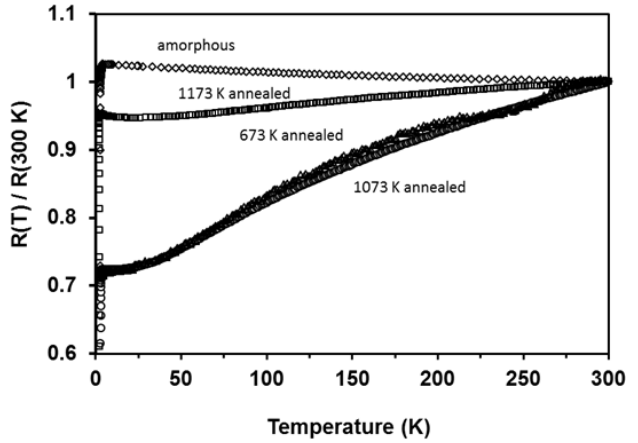

Figure 3a. The relative resistivity ($\rho(T)/\rho(300K)$): amorphous (◊), 673K annealed (□), 1073K annealed (○), 1173K (Δ)

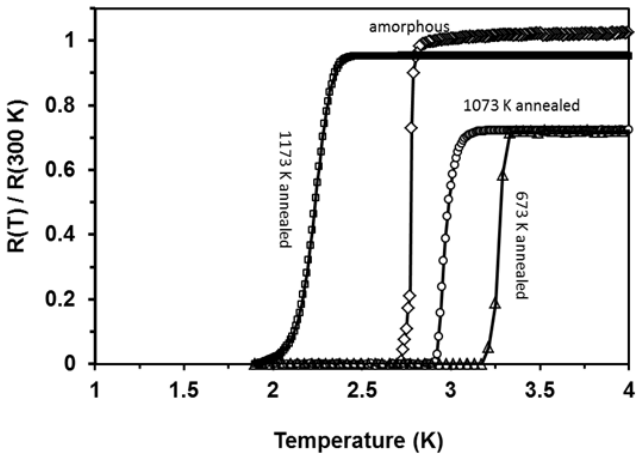

Figure 3b. enlargement of part of the data in Figure 3a

We have chosen to compare the 1073K annealed sample with the amorphous state since 1073K is well beyond T_x which grantees full crystallization. Figure 4 shows the behavior of T_c upon increasing the applied magnetic fields for the amorphous and the 1073K annealed samples. The rate of change of the applied field with temperature at T_c $(\partial H_{c2}/\partial T)_{Tc}$ was determined in the same way as Altounian *et al* [1]. It was found to be -3.1T/K and -1.86T/K for the amorphous and fully crystallized state respectively. $(\partial H_{c2}/\partial T)_{Tc}$ for the superconducting state in the crystallized state decreases faster than the amorphous state, an indication that the superconducting phase in the fully crystallized state has less pining sites and less defects than the amorphous state. In accordance with the extended Ginzburg-Landau-Abrikosov-Grokov (GLAG) theory [19]: $(\partial H_{c2}/\partial T)_{Tc} = -\eta(4k_B e/\pi)\rho N(E_F)$ where k_B is the Boltzmann constant, e is the electronic charge, ρ is the electrical resistivity, $N(E_F)$ is the density of states at the Fermi surface and η is an enhancement factor that takes a value of 1 for weak-coupling superconductors [20]. From the above equation $N(E_F)$ was determined to be 1.7e V^{-1} $atom^{-1}$ and 2.8 eV^{-1} $atom^{-1}$ for the amorphous and fully crystallized states respectively. These values are listed in Table 1. The fully crystallized state has more density of states at the Fermi surface which may indicate stronger electron-phonon coupling in comparison with the amorphous state. $(\partial H_{c2}/\partial T)_{Tc}$ can be also expressed as $(\partial H_{c2}/\partial T)_{Tc} = -\eta(4k_B/\pi eD)$, where D is the electron diffusivity and equal to $\upsilon_F l/3$ where υ_F the Fermi velocity and l is the mean free path. D was found to be 5.9 x $10^{-5}m^2$ s^{-1} for the fully crystallized state and 3.5 x $10^{-5}m^2$ s^{-1} for the amorphous state. The fully crystallized state has a larger electronic diffusivity and most likely longer electronic mean free path which may explain the lower resistivity. Furthermore, the zero temperature coherence length (ξ_0) can be expressed in terms of $(\partial H_{c2}/\partial T)_{Tc}$ according to the following equation $\xi_0 = 1.81 \times 10^{-8} \times [T_c \times (\partial H_{c2}/\partial T)]^{-1/2}$ [21]. The estimated values for ξ_0 were found to be 77 Å and 62 Å for the fully crystallized and amorphous state respectively as listed in Table 1. This indicates that the fully crystallized state is more homogeneous and has fewer defects.

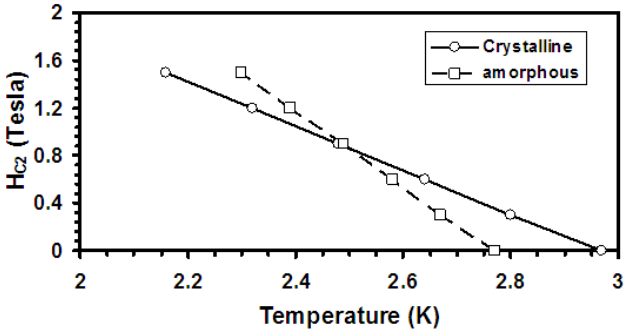

Figure 4. H_{c2} as a function of T_c for the amorphous (squares) and the 1073K annealed (circles) metallic glass at low temperatures

Table 1. The room temperature resistivity ρ(300K), T_c, temperature gradient $(-\partial H_{c2}/\partial T)_{Tc}$ near T_c, the electron diffusion constant D, the zero temperature coherence length ξ_0, and density of states $N(E_F)$

	amorphous	crystallized
ρ(300K) ± 5 (μΩ cm)	165	60
T_c ±0.01 (K)	2.77	2.97
$(-\partial H_{c2}/\partial T)_{Tc}$ ±0.1 (T/K)	3.1	1.86
D ±0.1(x $10^{-5}m^2$ s^{-1})	3.5	5.9
ξ_0 ±5 (Å)	62	77
$N(E_F)$ ±0.1 (eV^{-1} $atom^{-1}$)	1.7	2.8

4. Discussion

Previous studies on $Fe_{0.2}Zr_{0.8}$ and $Co_{0.2}Zr_{0.8}$ metallic glasses have resulted in an enhancement in T_c upon annealing [9,11]. The annealing temperatures in these studies were below T_x where the amorphous state was thermally relaxed. The enhancement in T_c was attributed to the decrease of the spin fluctuation mass enhancement factor (λsf) in the modified McMillan equation [10]. In the present study the annealing temperature is higher than Tx and the whole metallic glass is fully nano-crystallized; hence; the existence of any amorphous phases within the annealed $Ni_{0.5}Fe_{0.5}Zr_3$ metallic glasses is ruled out. Yet we see clear enhancement in Tc even when the annealing temperature is 1073K well beyond T_x. The 1073K annealed sample contains different crystalline phases of Fe-Zr and Ni-Zr, some of these phases are metastable such as fcc $FeZr_2$ and fcc $NiZr_2$ in addition to the more stable C16 Zr_2Ni and Zr_2Fe. The intermetallic C16 crystalline compounds Zr_2Ni and Zr_2Fe display superconductivity at 1.58K and 0.17K respectively [14,15,16]. These values are not even comparable to the observed Tc of 2.97 for the 1073K annealed sample. We would like to think that the metastable fcc $FeZr_2$ and $NiZr_2$ are responsible for the enhancement in Tc for the 673 and 1073K annealed samples. Further annealing at 1173K removed the metastable fcc $FeZr_2$ and $NiZr_2$ phases. The observed Tc of 2.23K for the 1173K annealed sample compares well with that of 2.44K for the C16 $Ni_{0.5}Fe_{0.5}Zr_2$ [22] The crystallization process of the $Ni_{0.5}Fe_{0.5}Zr_3$ metallic glass favors the formation of metastable phases on the way to more stable phases. Liu et al has found that the crystallization evolution in FeZr2 follows the sequence of fcc $FeZr_2$ then fcc $FeZr_2$ + bct $FeZr_2$ then bct $FeZr_2$ [23], this is in support of our findings. We would like to suggest that the T_c of the metastable phases varies with variations in the size of the nano crystallites, the lattice parameters and composition as the metastable phases evolves toward more stable phases. For this reason, we have observed a higher T_c for 673K annealed sample. It seems that the formation of metastable phases in some metallic glasses during the crystallization process could lead to enhancement in T_c, and we may suggest that this could happen even if the majority of the metallic glass is in the amorphous state as long as the number of metastable nano crystallites are sufficient enough to form a superconducting path.

5. Conclusions

The resistivity temperature dependence of the amorphous and crystallized states of the $Ni_{0.5}Fe_{0.5}Zr_3$ metallic glass was investigated over the temperature range 2-300K. The resistivity of the amorphous state was explained within the frame work of Mizutani's empirical formula as group four metallic glasses with d electrons at the Fermi energy level. DSC analyses rivaled that the present metallic glass has crystallization temperature of 660k. Samples of the $Ni_{0.5}Fe_{0.5}Zr_3$ metallic glass were annealed at temperatures higher than 660K. The 673 and 1073K annealed metallic glasses displayed a peculiar resistivty versus temperature behavior. At low temperatures, the amorphous and the crystallized states were found to be superconducting. Enhancement in T_c was observed for The 673 and 1073K annealed metallic glasses.

Acknowledgement

The author would like to acknowledge the support of equipment grant from UAE University and individual research grant (grant# 01-02-2-11/09) from research affairs at UAE University.

References

[1] Altounian , Z., and J. O. Strom-Olsen, J. O., "Superconductivity and spin fluctuations in M-Zr metallic glasses (M=Cu, Ni, Co, and Fe)" *Phys. Rev. B* 27. 4149-4156. 1983.

[2] Batalla, E., Altounian, Z., and J. O. Strom-Olsen, J. O., "Magnetism and electron-mass enhancement in zirconium-rich Fe-Zr and Co-Zr metallic glasses" *Phys. Rev. B* 31. 577-580. 1985.

[3] Mizutani, U., "Electronic structure of metallic glasses" *Prog. Mater. Sci.* 28. 97-228. 1983.

[4] Mizutani, U., "Systematic studies of electron transport properties of metallic glasses," in *Proceedings of the Fifth International Conference on Rapidly Quenched Metals*, North-Holland, 977-980.

[5] Mizutani, U., "Electron transport properties of non-magnetic metallic glasses" *Mater. Sci. Eng.* 99. 165-173. 1988.

[6] Mizutani, U., Tanaka, M., and Sato, H., "Studies of negative TCR and electronic structure of nonmagnetic metallic glasses based on Y and La" *J. Phys. F: Met. Phys.* 17. 131-142. 1987.

[7] Altounian, Z., Dantu, S. V., and Dikeakos, M., "Effects of spin fluctuations on the resistivity of metallic glasses" *Phys. Rev. B* 49. 8621-8626. 1994.

[8] Hamed, F., Razavi, F. S., Bose, S. K., and Startseva, T., "Spin fluctuations in metallic glasses $Zr_{75}(Ni_xFe_{1-x})_{25}$ at ambient and higher pressures " *Phys. Rev. B* 52 9674-9678. 1995.

[9] Sabouri-Ghomi, M., and Altounian, Z., "Enhancement of superconductivity in relaxed Fe-Zr metallic glasses" *J. Non-cryst. Solids* 205-207. 962-965. 1996.

[10] Daams, J. M., Mitrovic, B., and Carbotte, J. P., "Simulation of the Effects of Paramagnons on a Superconductor by a Simple Rescaling" *Phys. Rev. Lett.* 46. 65- 68. 1981.

[11] Kokanović, I., Leontić, B., Lukatela, J., and Tonejć, A., "The effect of thermal-relaxation on the short-range order in $Zr_{80}Co_{20}$ metallic glass" *Mater. Sci. Eng. A* 375-377. 688-692. 2004.

[12] Kokanović, I., "Effect of disorder on the electrical resistivity in the partially crystalline $Zr_{76}Ni_{24}$ metallic glasses" *J. alloys and compd.* 421. 12-18. 2006.

[13] Mattias, B. T., Geballe, T. H., and Compton, V. B., "superconductivity" *Rev. Mod. Phys.* 35 1-22. 1963.

[14] Havinga, E. E., Damsna, H., and Kanis, J. M., "Compounds and pseudo-binary alloys with the $CuAl_2$ (C16)-type structure I. Preparation and X-ray results" *J. Less-common Met.* 27 (2). 169-186. 1972.

[15] McCarthy, S. L., "The superconductivity and magnetic susceptibility of some zirconium-transition-metal compounds; evidence for an anticorrelation" *J. Low Temp. Phys.* 4 (5). 489-501. 1971.

[16] Salinke, H., G., Das, G. P., Raj, P., Sahni, V. C., and Dhar, S. K., "Band filling and superconductivity in Zr_2M compounds" *Physica C* 226. 385-390. 1994.

[17] Nava, F., Bisi, O., and Tu, K. N., "Electrical transport properties of V_3Si, V_5Si_3, and VSi_2 thin films" *Phys. Rev. B* 34. 6143-6150. 1986. And references therein.

[18] Kanemaki, S., Takehira, O., Fukamichi, K., and Mizutani, U., "Low-temperature specific heats and magnetic properties of $Co_{100-x}Zr_x$ metallic glasses over a wide concentration range x=10-80" *J. Phys. F: Condens. Matter* 1. 5903-5913. 1989.

[19] Eilenberger, G., and Ambegaokar, V., "Bulk (H_{c2}) and Surface (H_{c3}) Nucleation Fields of Strong-Coupling Superconducting Alloys" *Phys. Rev.* 158. 332-339. 1967.

[20] Rainer, D., and Bergmann, G., "Temperature dependence of H_{c2} and κ_1 in strong coupling superconductors" *J. Low Temp. Phys.* 14 (5-6). 501-519. 1974.

[21] Kes, P. H., and C. C. Tsuei, C. C., "Two-dimensional collective flux pinning, defects, and structural relaxation in amorphous superconducting films" *Phys. Rev. B* 28. 5126-5139. 1983.

[22] Amamou, A., Kuentzler, F., Dossmann, Y., Forey, P., J. L. Glimois, J. L., and Feron, J. L., "Electronic structure and electron-phonon coupling in the Ni-Zr system" *J. Phys. F: Met. phys.* 12. 2509-2522. 1982.

[23] Liu, X. D., Liu, X. B., and Altounian, Z., "Structural evolution of $Fe_{33}Zr_{67}$ and $Fe_{90}Zr_{10}$ metallic glasses" *J. Non-cryst. Solids*, 351. 604-611. 2005.